MABS
2018, VOL. 10, NO. 8, 1322–1331
https://doi.org/10.1080/19420862.2018.1506648

Taylor & Francis
Taylor & Francis Group

REPORT

A minimal physiologically based pharmacokinetic model to investigate FcRn-mediated monoclonal antibody salvage: Effects of K_{on}, K_{off}, endosome trafficking, and animal species

Brian M. Maas and Yanguang Cao

Division of Pharmacotherapy and Experimental Therapeutics, UNC Eshelman School of Pharmacy, University of North Carolina at Chapel Hill, Chapel Hill, USA

ABSTRACT

Manipulation of binding affinity between monoclonal antibodies (mAbs) and the neonatal Fc receptor (FcRn) has been leveraged to extend mAb half-life; however, the steps required for success remain ambiguous and experimental observations are inconsistent. Recent models have considered the time course of endosomal transit a major contributor to the relationship between FcRn affinity and antibody half-life. Our objective was to develop a minimal physiologically based pharmacokinetic model to explain how changes in IgG-FcRn association rate constant (K_{on}), dissociation rate constant (K_{off}), and endosomal transit time [$T_{(w)}$] translate to improved IgG clearance across mice, monkeys and humans. By simulating mAb clearance across physiological values of K_{on}, K_{off}, and $T_{(w)}$, we found that lowering K_{off} improves clearance only until the dissociation half-life reaches endosomal transit time. In contrast, K_{on} influenced clearance independently of $T_{(w)}$.The model was then applied to fit 66 mAb plasma profiles across species digitized from the literature, and clearance of mAb (CL_{IgG}) and vascular fluid-phase endocytosis rate (CL_{up}) were estimated. We found that CL_{IgG} scaled well with body weight (allometric exponent of 0.90). After accounting for mAbs with significant FcRn binding at physiological pH, CL_{up} was allometrically scalable (exponent 0.72). For the antibodies surveyed, K_{on} was more highly correlated with CL_{IgG} across all species. The relationship between K_{off} and K_D with CL_{IgG} was largely inconsistent. Taken together, this model provides a parsimonious approach to evaluate endosomal transit kinetics using only mAb plasma concentrations. These findings reinforce the idea that endosomal transit kinetics should be considered when modeling FcRn salvage.

ARTICLE HISTORY
Received 8 June 2018
Revised 19 July 2018
Accepted 26 July 2018

KEYWORDS
therapeutic antibody; endosomal transit; FcRn salvage; mPBPK; clearance

Introduction

Sales revenue of monoclonal antibodies (mAbs) represented half of that of all biopharmaceuticals in 2013, and their global sales are expected to reach $125 billion by 2020.[1] The most common isotype of therapeutic antibodies is immunoglobulin G (IgG).[2] Its extended half-life (~ 21 days) compared to other isotypes allows for less frequent dosing in patients. The primary reason for IgG plasma persistence is its ability to bind to the neonatal Fc receptor (FcRn, or Brambell receptor).[3] The major route of elimination for IgG is non-specific intracellular catabolism.[4] FcRn binds to IgG in a pH-dependent manner to protect it from lysosomal degradation and subsequently recycles it back to blood circulation. IgG is taken up into cells by non-specific fluid-phase pinocytosis and trafficked to the early endosome.[5] At physiological pH, IgG has a low affinity for FcRn, but as the endosome acidifies, IgG binds to FcRn with relatively higher affinity via a specific site on the Fc domain. Unbound IgG undergoes degradation in the lysosome, while IgG-FcRn complexes are efficiently recycled back to the cell surface where the complex dissociates at a physiological pH and releases IgG back to circulation.

This mechanism has been leveraged to increase the half-life of therapeutic mAbs by optimizing the strength at which IgG binds to FcRn in the acidic endosomal environment to rescue more antibody from intracellular degradation.[6,7] Some studies have shown a positive relationship between IgG half-life and increased FcRn binding at pH 6,[8,9] while results from other studies have yielded conflicting results.[3,5,10] Evidence also suggests that IgG-FcRn binding affinity at physiological pH is an important factor in driving antibody clearance.[11–13] FcRn-IgG binding affinity is linearly correlated with pH,[8] and achieving an appropriate affinity to balance lysosomal rescue without hindering release at physiological pH is important.[14] However, several other factors are thought to contribute to the relationship between FcRn affinity and IgG half-life, including species differences, FcRn tissue distribution, and endosomal binding kinetics.[5,14]

Many models describe IgG-FcRn interactions in terms of equilibrium binding coefficients (K_D). It has been proposed that the lack of correlation between equilibrium affinity and mAb pharmacokinetics (PK) occurs because the time course

CONTACT Yanguang Cao yanguang@unc.edu UNC Eshelman School of Pharmacy, UNC at Chapel Hill
Color versions of one or more of the figures in the article can be found online at www.tandfonline.com/kmab.
Supplemental data for this article can be accessed here.

of endosomal transit is too brief to allow binding to reach equilibrium.[15] The dissociation (K_{off}) half-life of antibodies ranges from 6 to 58 minutes, while endosomal trafficking duration half-life has been approximated at 7.2 minutes.[16–18] The actual time that FcRn and IgG have to bind under acidic conditions is likely even shorter, due to the gradual acidification within the maturing endosomes.[15]

Chen and colleagues designed a catenary physiologically based pharmacokinetic (PBPK) model[15] that incorporates the time-course of FcRn binding and endosome transit, which more accurately predicted IgG PK than similar published equilibrium models.[19,20] This model suggested that modulating the association rate constant (K_{on}) rather than decreasing K_{off} has a larger effect on mAb systemic clearance. To further investigate the factors most influential in affecting mAb PK, we developed a minimal PBPK (mPBPK) model by grouping components of the full PBPK model previously established for IgG, and surveyed the PK of mAbs that have measured *in vitro* FcRn binding parameters. We aimed to build on previous findings by employing a more parsimonious approach to estimate critical model parameters for several species using *in vivo* PK data from the literature, while accounting for IgG-FcRn binding differences at acidic and physiological pH. Herein, we present a mPBPK model that accounts for mAb-FcRn binding, endosomal trafficking, and species differences to improve the understanding of important factors in translating FcRn binding affinity to mAb half-life.

Results

The mPBPK model takes a reductionist approach to simplify full PBPK models, using factors that are most relevant to mAb PK. It retains basic physiological information (e.g., plasma/tissue volumes, systemic lymph flow) in model assumptions to provide more physiologically relevant parameters than mammillary models. It also provides concentrations of mAbs in two groups of tissues by solely analyzing plasma concentration-time data. The average tissue concentrations often represent mAb concentrations at sites of action. This is especially critical in clinical situations when only plasma concentrations data is available. This analysis was conducted by extending our previous mPBPK model with considerations for endosome trafficking dynamics and recycling. The concentrations of FcRn in endosomes are much higher than the concentrations of therapeutic antibodies, which supports a constant FcRn concentration assumption and linearization of the FcRn-antibody binding system. Linear approximation of IgG-FcRn binding kinetics enables an explicit review and evaluation of critical factors contributing to IgG systemic clearance.

First, a local sensitivity analysis was conducted to assess model behavior and stability. Equation (1) was used to simulate CL_{IgG} across plausible ranges of K_{on} (550 to 2×10^6 1/Ms), K_{off} (1×10^{-5} to 1.0 1/s), and transit time (20 to 800 sec). The simulated ranges for binding constants were selected from literature reported ranges for antibody-antigen association and dissociation rate constants,[21] which included measured ranges of IgG-FcRn binding constants.

$$\mathrm{CL_{IgG}} = \mathrm{CL_{up}} \cdot \left[\frac{\mathrm{C}}{\mathrm{B}+\mathrm{C}} + \frac{\mathrm{B}}{\mathrm{B}+\mathrm{C}} \cdot \mathrm{e}^{-(\mathrm{B}+\mathrm{C})\cdot \mathrm{T(W)}}\right] \quad (1)$$

where CL_{up} is the uptake rate of IgG into the endosome by fluid-phase endocytosis. $\mathrm{B} = \mathrm{K_{on}}\,[\mathrm{FcRn}]_{\mathrm{TA}}$ and $\mathrm{C} = \mathrm{K_{off}}$, $[\mathrm{FcRn}]_{\mathrm{TA}}$ is effective FcRn concentration available for therapeutic antibodies

Figure 1A shows that a decline in K_{off} would decrease mAb clearance until the dissociation half-life reaches endosomal transit time. Further decreases in K_{off} beyond this point failed to affect mAb clearance, particularly at brief endosomal durations. Figure 1B suggests that increases in K_{on} would decrease the clearance of antibody, regardless of the endosomal transit duration. Figure 1C shows that when the effect of K_{off} on mAb clearance has plateaued, K_{on} becomes the primary driver of clearance, and further increasing of it produces reductions in antibody clearance.

Next, the literature was surveyed and a total of 86 mAb PK profiles with paired FcRn binding affinities from 16 publications were identified. Twenty profiles (Supplement Table 1) used radioactivity to measure whole body mAb exposure as opposed to plasma concentrations and could not be analyzed to extract accurate estimates of clearance. The remaining 66 plasma PK profiles (Supplemental Table 2) were digitized and fit to the developed mPBPK model, and a total of 43 profiles (10 mouse, 20, monkey, and 13 human) were well-described by the model. All parameters were estimated with good precision (CV < 25%). Non-compartmental analysis (NCA) was further performed on profiles that were not adequately described by the model or were described with unreasonable

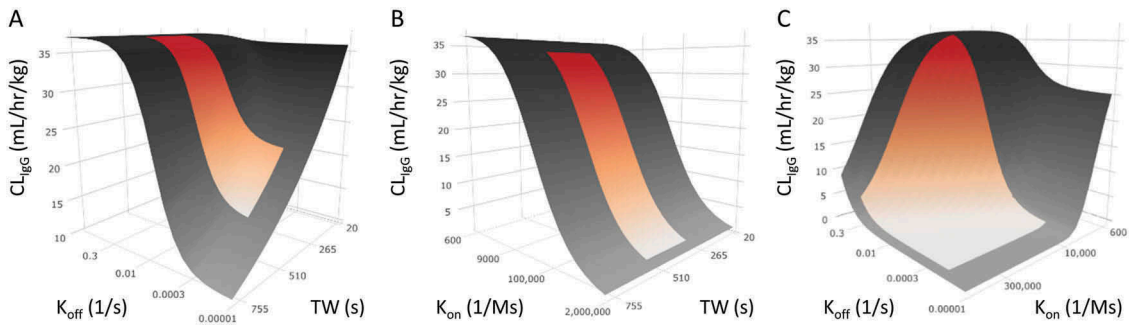

Figure 1. Simulation of monoclonal antibody (mAb) clearance across physiological ranges of IgG-FcRn binding affinity and endosomal transit time. **(A)** mAb clearance vs. K_{off} and $T_{(w)}$. **(B)** mAb clearance vs. K_{on} and $T_{(w)}$. **(C)** mAb clearance vs. K_{off} and K_{on}. Colored regions represent parameter ranges from mAb survey from the literature. Abbreviations: K_{on} association rate constant; K_{off} dissociation rate constant; $T_{(w)}$ endosomal transit time; CL_{IgG} clearance of immunoglobulin G.

parameter estimates to ensure exclusion of those profiles did not affect our findings. Results from our analysis using an NCA-based approach to impute missing clearance estimates is provided in the supplementary material. Estimates of vascular reflection coefficient σ_1 averaged 0.96 (range 0.93 to 0.99) and estimates of σ_2 averaged 0.81 (range 0.26 to 0.97), both of which agree with previous publications.[22] When digitized data did not support a reasonable estimation of σ_1, it would be fixed to a commonly reported value of 0.95 or 0.99,[23] based on best model fit. Mean ± standard deviation (SD) estimates for CL_{IgG} (mL/hr/kg) were 0.436 ± 0.332 for mouse, 0.183 ± 0.145 for monkey, and 0.168 ± 0.068 for human. Values for CL_{up} were calculated according to Equation (1) using CL_{IgG} estimates and known IgG-FcRn binding affinities. Mean ± SD values for CL_{up} (mL/hr/kg) were 11.8 ± 16.8 for 25 g mouse, 142 ± 312 for 3.3 kg monkey, and 1.43 ± 3.81 for 70 kg human.

Since IgG-FcRn binding is not appreciable at physiological pH, measurements of binding affinity are often not reported. Knowing that FcRn-IgG binding affinity is linearly correlated with pH,[8] K_D values across a range of pH values were digitized from the literature,[8,12] log-transformed, and normalized to their K_D value at pH of 6. A simple linear regression model was fit to determine the slope of the relationship.

$$\ln(K_{D\,7.4}) = 3.22 \cdot pH - 19.2 \quad (2)$$

For each antibody surveyed, K_D at pH 7.4 was projected using the fitted slope and the known K_D value at pH 6. This relationship was used to identify antibodies from the dataset with substantial FcRn affinity at pH 7.4, which may impede their effective release back into circulation after FcRn salvage. Figure 2 shows the estimates of CL_{up} for antibodies above and below the binding threshold of 860 nM at physiological pH. Six antibodies had predicted K_D values above this threshold and demonstrated considerably higher estimates for CL_{up} within the monkey species. These six antibodies estimates were subsequently excluded from calculation of the CL_{up} summary statistics. Exclusion of these antibodies from the estimates of CL_{up} yielded a mean of 2.09 mL/h/kg and a SD of 2.87 in monkey.

To assess allometric scalability, estimates for CL_{IgG} and CL_{up} were fit to the equation $y = bx + a$, where y is the log-transformed clearance estimate, x is the log-transformed species weight, b is the allometric exponent, and a is the intercept. CL_{IgG} estimates scaled well with body weight, yielding an allometric exponent of 0.90 (Figure 3A). CL_{up} values did not initially scale with body weight due to the large variability within the monkey species (Figure 3C), but were scalable (allometric exponent of 0.72) after exclusion of mAbs with strong FcRn binding at pH 7.4 (Figure 3D).

Finally, CL_{IgG} estimates from surveyed mAbs were examined to determine which measures of FcRn binding affinity best explained the variability observed in the estimates. Figure 4 summarizes relationships between estimates of CL_{IgG} and reported K_{on}, K_{off}, and K_D. Antibodies with larger values of K_{on} consistently exhibited lower rates of clearance for all species. The correlation was stronger with monkey (Pearson $r = -0.92$) and mouse ($r = -0.75$) than for human ($r = -0.13$). Antibodies with lower K_{off} measurements displayed higher rates of systemic clearance in monkey ($r = -0.7$), which was unexpected. Overall, both K_{off} and K_D showed poor relationships with clearance, particularly K_D ($r = 0.13$ for mouse, $r = -0.16$ for monkey, $r = -0.21$ human).

Discussion

It is known that FcRn contributes to plasma persistence of mAbs (i.e., IgG); however, the changes in mAb half-life have not been explained by pH-dependent IgG-FcRn binding affinity alone.[5] Most models attempting to describe changes to mAb clearance have not considered endosomal trafficking in IgG-FcRn binding kinetics, even though the brief endosomal transit time likely does not allow for IgG-FcRn binding to achieve equilibrium. To this point, we developed a mPBPK model that incorporates FcRn binding affinity and endosomal trafficking to better understand the relationships between IgG-FcRn binding and mAb half-life across animal species. This approach allows us to investigate the parameters most critical to mAb clearance using only plasma concentrations extracted from the literature. The concept of this model is similar to the catenary model developed by Chen and

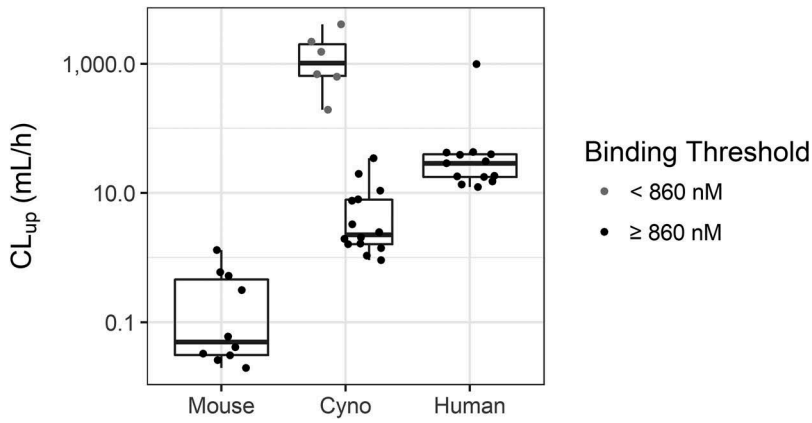

Figure 2. Estimates of CL_{up} for mouse, cynomolgus monkey, and human species. Gray points represent antibodies with predicted K_D at physiological pH of less than 860 nM. Black points represent antibodies with predicted K_D at physiological pH of greater than or equal to 860 nM. Abbreviations: CL_{up} endosomal uptake rate.

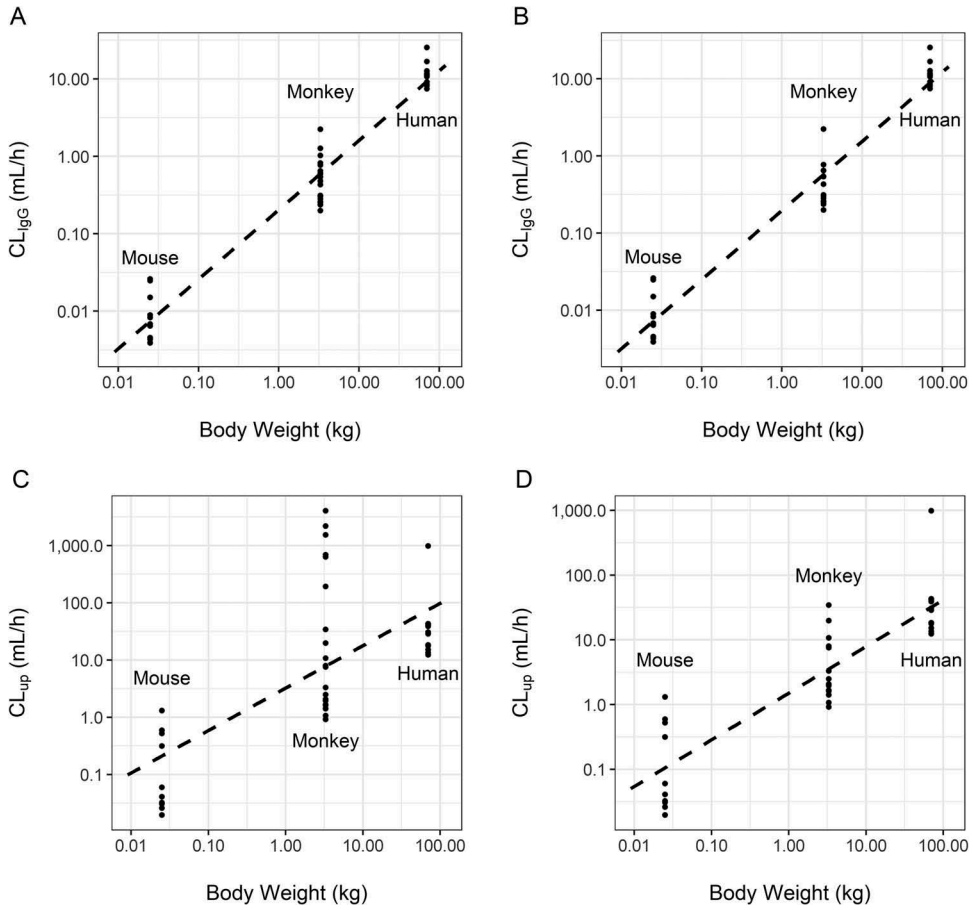

Figure 3. Allometric scaling of CL_{IgG} and CL_{up} across body weight. **(A)** CL_{IgG} vs. body weight. **(B)** CL_{IgG} vs. body weight for mAb with predicted K_D at physiological pH ≥ 860 nM. **(C)** CL_{up} vs. body weight. **(D)** CL_{up} vs. body weight for mAb with predicted K_D at physiological pH ≥ 860 nM. Black points represent individual clearance values and black lines show the results of simple linear regression to estimate the allometric exponent. Abbreviations: CL_{IgG} clearance of immunoglobulin G; CL_{up} endosomal uptake rate.

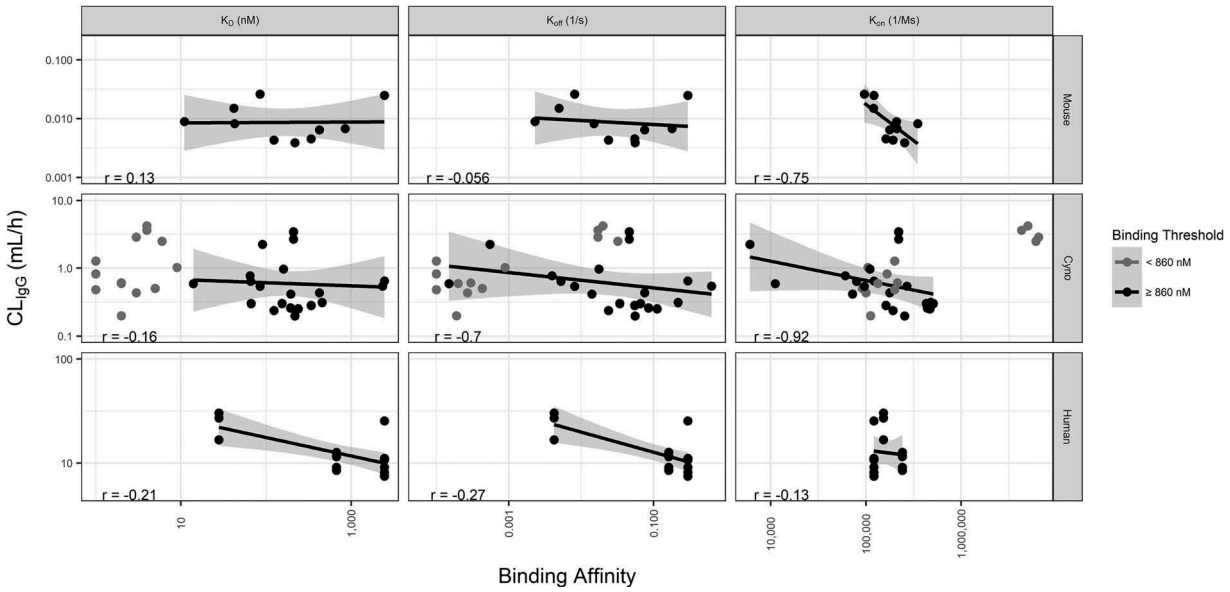

Figure 4. Relationships between CL_{IgG} and measures of binding affinity. Black and grey points represent surveyed mAbs with a predicted K_D at physiological pH of greater than or equal to 860 nM and less than 860 nM, respectively. Linear regression with 90% confidence intervals are shown with black lines and grey shaded regions, respectively. Abbreviations: K_{on} association rate constant; K_{off} dissociation rate constant; K_D equilibrium rate constant; CL_{IgG} clearance of immunoglobulin G.

colleagues,[15] but this model provides a more parsimonious and explicit approach that relies on linear approximations and supports estimation of physiologically relevant parameters with relatively high certainty.

The primary underlying assumption is that FcRn salvage efficiency, and therefore mAb clearance, is dictated by the fraction of IgG bound to FcRn at the time of endosomal sorting. This bound fraction is fundamentally determined by FcRn binding parameters K_{on}, K_{off}, and endosome transit [$T_{(W)}$]. As these factors do not influence mAb clearance independently, simulations were performed across physiological ranges of these parameters at endosomal pH to consider their interactions. Based on our model, all three parameters significantly affected mAb clearance. Decreasing K_{off} demonstrated a reduction in mAb clearance that was dependent on $T_{(W)}$. As the dissociation half-life approached the endosomal transit half-life, this effect plateaued and further lowering of K_{off} beyond this point failed to have any additional benefit to antibody clearance. Increases in K_{on} reduced mAb clearance in a manner that was independent of $T_{(W)}$. There was a strong interaction between the effects of K_{on} and K_{off} on mAb clearance that suggested both parameters are important contributors to FcRn salvage efficiency, as has been shown previously.[12] These results are in agreement with other publications, which showed that changes to K_{off} only resulted in up to a 1.5-fold improvement in half-life.[15] Historically, decreasing K_{off} to reduce K_D has been the standard approach taken during attempts to improve IgG half-life. Taken together, our simulations suggest that optimizing K_D will not always produce a reduction in mAb clearance due to limitations surrounding $T_{(W)}$, and that both K_{on} and K_{off} should be considered. These findings are reflected in Figure 1.

The survey of mAbs from published literature was used to validate our model, as concentration-time profiles were adequately described by the model across all species. Surveyed data also allowed the evaluation of clearance parameters (CL_{IgG} and CL_{up}). CL_{IgG} was estimated across species and was found to be allometrically scalable with an average exponent of 0.9. This value is consistent with our previously reported estimate for mAbs.[24] CL_{up} was calculated using estimates for CL_{IgG} and known values for K_{on} and K_{off} according to Equation (1). Some antibodies yielded CL_{up} values within the monkey species that were much larger (approximately 100-fold) than the remainder of estimates, resulting in a bimodal distribution. This cluster of values increased the mean CL_{up} in monkeys to more than 4-fold that observed in humans, which disallowed estimation of an allometric exponent.

An 'affinity threshold' at physiologic pH of 860 nM[13] has been described that suggests mAbs with increased IgG-FcRn binding at physiological pH demonstrated shorter half-lives, despite expected improvements from binding at pH 6. Research suggests antibodies with FcRn affinities below this threshold can efficiently be recycled back to the plasma, while antibodies with affinities above this threshold remain tightly bound to FcRn and are returned to the endosome for degradation. The concept of an affinity threshold has also been supported by others.[12] Our model assumes that all antibody clearance is determined entirely by the fraction of IgG bound to FcRn at the time of sorting. Antibodies with hindered FcRn release to plasma represent another route of clearance that violates our assumption and may contribute to the variability observed within the monkey CL_{up} estimates. We hypothesize that estimates of CL_{up} for mAbs with strong binding to FcRn at physiological pH are artificially high and result from the model attempting to compensate for increases in clearance not explained by IgG-FcRn binding kinetics in the sorting endosome.

To test this, we compared FcRn binding affinity at pH 7.4 for all surveyed antibodies to the affinity threshold described by others. Since measurements for FcRn binding at physiological pH were largely unavailable, we developed a linear regression model using published data[8,12] to predict K_D values at pH 7.4 for surveyed antibodies. Closer examination revealed that the six mAbs with unusually high estimates of CL_{up} exhibited binding affinities above the designated threshold. Collectively, these mAb had a median CL_{up} estimate that was almost 1,000 fold higher than that of the remaining antibodies (Figure 2). To account for this, antibodies predicted to have a K_D value of less than 860 nM at physiological pH were excluded from the calculation of CL_{up}. This adjustment greatly reduced the variability of the CL_{up} estimate within the monkey species and allowed the parameter to be properly scaled with body weight, resulting in an allometric exponent of 0.72.

Clearance mechanisms that are not considered in the developed model, such as Fcγ-dependent or target-mediated elimination, may add to the high variability observed in monkey CL_{up} estimates. Although all surveyed antibodies displayed linear clearance, a minor contribution of target-mediated elimination cannot be ruled out.

Simulations suggested FcRn binding affinity in terms of K_D does not drive antibody half-life alone. These findings were reinforced by examination of our survey results and the relationship between antibody clearance and measured K_{on}, K_{off}, and K_D values at pH 6. Across species, K_D appeared to explain the least amount of variability in antibody clearance, demonstrating almost no relationship with CL_{IgG}. The relationship between CL_{IgG} and K_{off} was also relatively weak and contrary to what was expected, as antibodies with lower K_{off} values tended to exhibit higher clearance for monkey and human species. Binding affinity in terms of K_{on} displayed the strongest relationship with CL_{IgG} across all species studies, although the range of K_{on} values for mAb data in humans was limited. We acknowledge that each of these parameters explains a relatively low amount of variability within CL_{IgG}, and it is likely that several other factors contribute to antibody clearance, including isoelectric point, charge balance, mAb aggregation, and target-mediated clearance.[4] However, these results still show that K_{on} should be an important consideration when translating FcRn binding affinity to mAb clearance.

Comparing data for antibodies across several studies with different methodologies proved challenging. The high variabilities seen in the results were likely due to factors such as different assay techniques, varying animal sizes, and inconsistent data reporting methods. As a consequence, a considerable number of surveyed mAbs could not be fit by the model (i.e., estimation failed to converge) or produced unreasonable parameter estimates, and were excluded from the final analysis. A representative sample of fits and diagnostic plots is provided in Supplemental Figure 1. Data should never be discarded without reason, and we felt inclusion of poorly fitted profiles would bias our clearance estimates and render

our results uninterpretable. Profiles from one study[25,26] were excluded because the majority of mAbs did not allow for model convergence. This raised concerns that the assay or study methodology did not meet our assumptions. Some profiles were systematically under-predicted by the model (Supplemental Figure 1B), which may be attributed to measurement error or variability in animal sizes and plasma volumes. These unusual profiles were also observed and summarized in our previous publication with sufficient explanation.[17] A complete list of digitized mAbs, including those excluded from the final analysis, is provided is Supplemental Table 2.

In an effort to ensure exclusion of mAb profiles did not affect our results, we conducted NCA to obtain mAb CL estimates for mAbs that could not be characterized by the model. Clearance estimates from NCA were then imputed for mAbs previously excluded, and the analysis was repeated for all 66 antibodies surveyed. Increased variability was observed in CL_{IgG} estimates obtained by NCA, supporting the advantage of estimating mAb CL with a model-based approach. While the exact cause of poorly-fitting profiles could not be identified, they may be associated with factors that are not yet considered by the developed model, such as disease, immune status, and body size.[27] Nevertheless, incorporation of excluded antibodies did not substantially affect the scalability of CL_{IgG} and CL_{up} (Supplemental Figure 2) or the relationship between FcRn binding affinity at pH 6 and CL_{IgG} across species (Supplemental Figure 3). Some sources of variability were more predictable. Although surface plasma resonance (SPR) was used to measure FcRn-IgG interactions in all cases, variations in the format of the assay (i.e., stoichiometry and orientation) can yield different binding affinity results.[28] The focus of this model was to explore IgG-FcRn binding kinetics in the endosomes, and it had no mechanism to account for pH-dependent binding. Consequently, surveyed antibodies with appreciable FcRn binding at physiological pH were excluded from the final analysis. This was done to isolate the effect of FcRn binding kinetics and endosomal transit on half-life without mAb clearance being affected by hindered release into plasma. The bimodal distribution observed in CL_{up} estimates in monkey was well-described by differences in binding affinity at physiological pH.

By surveying several mAbs from the literature, we developed an extended mPBPK model that describes the disposition of IgG in the body, taking into account endosomal transit and FcRn binding kinetics. The rate of endosomal uptake was estimated across species and scaled well with bodyweight, and K_{on} has been identified as an important factor for increasing the persistence of IgG. This model provides a valuable framework to better understand determinants of mAb clearance and aids in the development of antibodies with more optimal pharmacokinetic properties. Future work will aim to add further considerations for pH-dependent IgG-FcRn binding kinetics and target-mediated drug distribution.

Materials and methods

Extended minimal PBPK model

The structural model used for this investigation was based on the previously published second-generation mPBPK model for mAbs.[17,23] This model retains basic physiological information (e.g., plasma/tissue volumes, systemic lymph flow) and provides more physiologically relevant parameters than mammillary models. The mPBPK model also makes reasonable approximations of tissue concentrations of mAb by solely analyzing plasma concentrations-time data. The mPBPK model allows for a simplified and physiologically based PK analysis when the granularity of a full PKPB model is not necessary or not feasible. Modifications were made to include an endosomal compartment in parallel with the plasma compartment to study the influence of FcRn salvage kinetics on mAb clearance (Figure 5A). The differential equations of this model are provided in Supplemental material. The total amount of antibody within the endothelial endosome at a given time is relatively small and the transcytosis between the plasma and endothelial endosomes is thought to be rapid.[23] Therefore, the existence of this parallel compartment should not affect the distribution of antibody within the plasma compartment, and lysosomal degradation within this compartment should mimic clearance from the plasma. The predictability of a similar mPBPK model has been evaluated[29] and showed that inclusion of an endosomal compartment into a mPBPK model adequately predicted mAb PK with a broad range of clearances and without substantial influence on antibody distribution.

The proposed mechanism for IgG salvage by FcRn within the endosomal space is depicted in Figure 5B. IgG is taken up into the early endosomes from the plasma via non-specific fluid-phase pinocytosis at an uptake clearance (CL_{up}) rate. Following this, the endosome acidifies and IgG binds to FcRn. At the time of endosomal sorting, the fraction of IgG that remains unbound (F_{ELI}) is delivered to the lysosome and cleared from the body (CL_{IgG}). The bound fraction of IgG (F_{SAL}) is recycled back into the plasma by FcRn.[4]

In this model, FcRn salvage efficiency is primarily determined by the FcRn-bound fraction of IgG at the time of endosomal sorting. The bound fraction is influenced by the rate of FcRn-IgG binding (K_{on}, K_{off}) and the duration of endosome transiting/sorting ($T_{(w)}$). The following equations show the deviation process of F_{ELI} and F_{SAL} in terms of these factors. Following the rules of binding kinetics, the concentration of IgG and IgG-FcRn complex in the endosomes with respect to time (t), can be denoted by:

$$\frac{d[Ab]}{dt} = -K_{on} \cdot [FcRn]_{TA} \cdot [Ab] + K_{off} \cdot [AF]\ IC[Ab] = \frac{C_P \cdot CL_{up}}{V_{Endo}} = A \quad (3)$$

$$\frac{d[AF]}{dt} = K_{on} \cdot [FcRn]_{TA} \cdot [Ab] - K_{off} \cdot [AF]\ IC[AF] = 0 \quad (4)$$

where [IC] is the initial condition, [Ab] is IgG concentration in endosomes, [AF] is IgG-FcRn complex concentration in endosomes, V_{Endo} is the volume of endosomes and $[FcRn]_{TA}$ is effective FcRn concentration available for therapeutic antibodies (estimated to be 1,600 nM).[15]

Laplace transformation of Equations (3) and (4) yields:

$$s\overline{Ab} - A = -K_{on} \cdot [FcRn]_{TA} \cdot \overline{Ab} + K_{off} \cdot \overline{AF} \quad (5)$$

$$s\overline{AF} - 0 = K_{on} \cdot [FcRn]_{TA} \cdot \overline{Ab} - K_{off} \cdot \overline{AF} \quad (6)$$

Integration of Equations (5) and (6) gives:

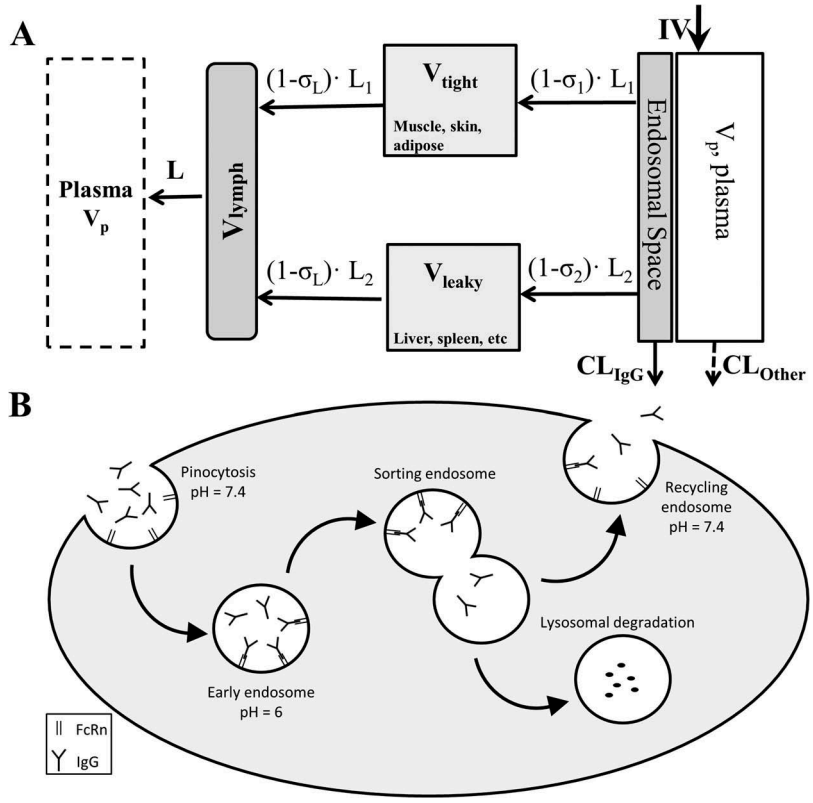

Figure 5. Extended mPBPK model **(A)** mPKPK model shown with endosomal compartment. The endosomal space is parallel to the plasma compartment and has a negligible volume. Antibody is taken up into the endosomal space at a rate of CL_{up} and cleared out of the body at a rate of CL_{IgG}. IgG is recycled back into the plasma at a rate of $CL_{up} - CL_{IgG}$. CL_{other} is assumed to be negligible in this modeling context. **(B)** FcRn salvage of IgG through the endosome. IgG is taken up into the early endosomes by fluid phase pinocytosis at a rate of CL_{up}. At the time of sorting, FcRn bound IgG will be sent to the RE and subsequently returned to the plasma. Unbound IgG will be cleared from the body via lysosomal degradation. Abbreviations: V_p plasma volume; V_{lymph} lymph volume; V_{leaky} leaky vasculature; V_{tight} tight vasculature; L lymph flow; σ reflection coefficient; IV intravenous; CL_{IgG} clearance of IgG; CL_{other} other clearance; CL_{up} endosomal uptake rate.

$$\overline{Ab}=\frac{A\cdot(s+K_{off})}{s^2+s\cdot\left(K_{on}\cdot[FcRn]_{TA}+K_{off}\right)} \tag{7}$$

Substituting $\alpha = 0$ and $\beta = K_{on}[FcRn]_{TA}+K_{off}$ provides:

$$\overline{Ab}=\frac{A\cdot(s+K_{off})}{(s+\alpha)\cdot(s+\beta)} \tag{8}$$

$$[Ab]=\frac{A\cdot(K_{off}-\alpha)}{\beta-\alpha}e^{-\alpha\cdot t}+\frac{A\cdot(K_{off}-\beta)}{\alpha-\beta}e^{-\beta\cdot t}$$
$$=\frac{A\cdot K_{off}}{\beta}+\frac{A\cdot(K_{off}-\beta)}{-\beta}e^{-\beta\cdot t} \tag{9}$$

By allowing $B = K_{on}\cdot[FcRn]_{TA}$ and $C = K_{off}$, the equation for concentration of unbound antibody in the endosome at a given time is:

$$[Ab]=A\cdot\left[\frac{C}{B+C}+\frac{B}{B+C}\cdot e^{-(B+C)\cdot t}\right] \tag{10}$$

The fraction of IgG salvaged by FcRn is:

$$F_{SAL}=1-\left[\frac{C}{B+C}+\frac{B}{B+C}\cdot e^{-(B+C)\cdot t}\right] \tag{11}$$

The duration IgG residing in endosomes will be the average lifespan of endosomes $T_{(W)}$. Then, the FcRn-bound fraction, at the time of endosome sorting into lysosomes will be:

$$F_{SAL}=1-\left[\frac{C}{B+C}+\frac{B}{B+C}\cdot e^{-(B+C)\cdot T(W)}\right] \tag{12}$$

Per the assumption that all IgG not bound to FcRn will undergo lysosomal degradation, the systemic clearance (CL_{IgG}) of IgG will be determined by Equation 1 (see Results).

Other models have suggested that endogenous antibodies may compete with therapeutic mAbs for FcRn, altering the PK of IgG.[12] We assume that FcRn binding capacity is not saturable at therapeutic concentrations of IgG. Several full PBPK models have estimated total FcRn concentration to be 33.0 ~ 49.8 μM,[20,30] which is approximately 1000-folder higher than endogenous IgG concentrations in plasma (10–15 mg/mL). Only extremely high doses of IVIG (~ 2000 mg/kg) have noticeable effects on the half-life of IgG.[31] This suggests that the available capacity for FcRn binding, at normal endogenous IgG concentrations, is much higher than the concentrations of therapeutic antibodies and supports our assumption that the binding between therapeutic IgG and FcRn could be considered a linear process.

Model simulation

Using Equation (1), a local sensitivity analysis was performed on critical model parameters (endosomal transit time and FcRn-IgG binding affinity at pH 6) to explore their influence on CL_{IgG}. Because the effect of one parameter on CL_{IgG} may be dependent

on the value of another, pairs of parameters were simulated simultaneously over a physiological range – K_{off} and $T_{(w)}$, K_{on} and $T_{(w)}$, and K_{on} and K_{off}.

Survey of antibody clearance

A literature search for PK profiles of IgG in mice, monkeys, and humans was conducted. Profiles from antibodies that displayed linear PK at observed doses and had FcRn binding affinity data reported in terms on K_{on} and K_{off} from SPR were included. These concentration-time profiles were digitized using WebPlot Digitizer v3.11 (Austin, Texas) and fit to our model using ADAPT5 (BMSR, Los Angeles, CA).

Physiological parameters and their values are listed in Table 1 and were fixed in the model. CL_{IgG}, σ_1, and σ_2 were estimated for each antibody based on extracted PK data. In cases where both reflection coefficients could not be accurately estimated, σ_1 was fixed to 0.95 or 0.99, two commonly used values found in literature.[23] Estimated values of CL_{IgG} and reported mAb-FcRn binding affinities were used in Equation (1) to determine CL_{up}. Values of CL_{up} were compared across species to assess whether this parameter scaled allometrically with body weight.

Relationships between CL_{IgG} and K_{on}, K_{off} and K_D

The relationship between FcRn binding affinity and antibody clearance and *was* explored by comparing K_{on}, K_{off}, and K_D to CL_{IgG} and quantified using linear regression.

The focus of this model was to explore factors related to IgG-FcRn binding kinetics within the endosome; however, studies have shown that FcRn binding affinity at physiological pH influences antibody salvage back to the plasma.[8] This model does not inherently account for pH-dependent binding. To investigate whether IgG-FcRn binding at physiological pH affected model estimates, we compared CL_{up} estimates between antibodies with strong and weak FcRn binding at pH 7.4. Most mAbs do not appreciably bind to FcRn at pH 7.4 and K_D values are rarely reported. Data for IgG-FcRn binding affinity across a range of pH values were extracted from the literature[8,12] and fit to a simple linear regression model (Figure 6). This linear model was then used to project K_D of surveyed antibodies at pH 7.4.

An IgG-FcRn affinity of 860 nM at pH 7.4 has been described as a threshold that determines mAb recycling efficiency.[13] It is thought that antibodies with affinities below this threshold can be efficiently released back into the plasma following FcRn salvage, but antibodies with affinities above leads to more rapid clearance. Antibodies that bind to FcRn with an affinity

Table 1. Model parameters estimates. Physiological parameters across species were obtained from the literature. CL_{IgG} was estimated from model fitting. CL_{up} was calculated based on known experimental values of K_{on} and K_{off}. CL_{other} was assumed to be negligible in this context.

Parameter	Definition	Value	Source (reference)
V_p	Plasma volume	4.5% of BW, 3.0 L/70kg human	[24]
V_L	Lymph volume	5.2 L for 70kg human, varied	[24]
V_{ISF}, V_{leaky}, V_{tight}	Interstitial fluid volume	Total:15.8 L; V_{leaky} 65%; V_{tight} 35%	[24]
L, L_1, L_2	Lymph flow	2.9 L/day; L_1 33%; L_2 67%	[24]
σ_1, σ_2, σ_L	Vascular and lymphatic reflection coefficients	σ_L = 0.2; σ_1 = 0.950 for V_{tight}; σ_2 = 0.710 for V_{leaky}	[22]
K_{on}, K_{off}	IgG:FcRn binding kinetics	Experimental Values	Literature (Table S1 and S2)
$T_{(W)}$	Duration of Endosomal trafficking	7.2 min	[16–18]
FcRnTA	Total Available FcRn	1,660 nM	[15]
CL_{up}	Fluid-phase endocytosis	$CL_{up} = CL_{IgG}/(1\text{-}F_{SAL})$	Calculated (Table S2)
CL_{IgG}	Antibody lysosome clearance	Estimated	Estimated (Table S2)
CL_{other}	Antibody non-lysosome clearance	Fixed to 0	N/A

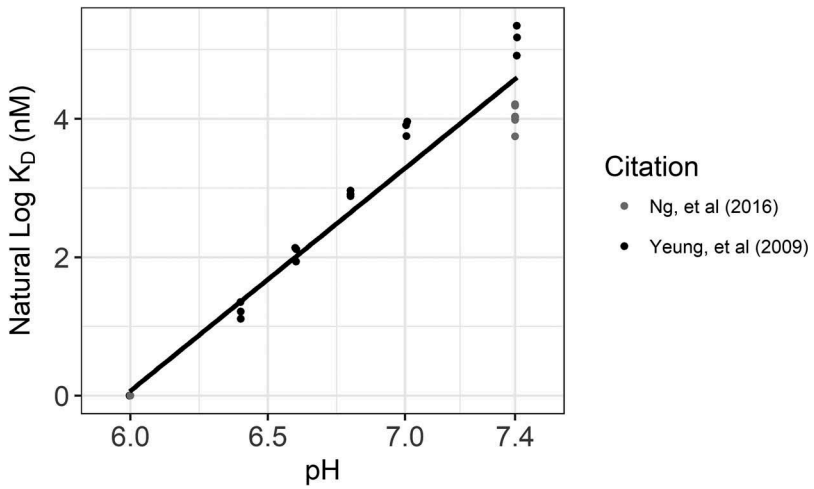

Figure 6. Normalized FcRn equilibrium binding affinity vs. pH. Antibody FcRn binding affinities at a range of pH values were digitized from the literature, normalized, and fit to a linear regression model. Black and grey points represent mAb digitized from Yeung, et al (2009)[8] and Ng, et al (2016),[12] respectively. Results from linear regression are depicted with the black line. Abbreviations: K_D equilibrium rate constant.

stronger than 860 nM at physiological pH were excluded in the calculation of CL_{up}, and analyzed separately when examining the correlation between CL_{IgG} and FcRn binding affinity.

Acknowledgments

This work was supported by NIH R35 GM119661 research grant. The authors would like to thank Rong Deng (Genentech, Inc.) for fruitful discussions and valuable suggestions on our research methods and manuscript development. They would also like to thank Xiaobing Li and Can Liu for assisting with non-compartmental analysis of antibodies.

Disclosure of Potential Conflicts of Interest

The authors have nothing to declare regarding conflict of interest with respect to this manuscript. BMM now works for Merck & Co., Inc.

Funding

This work was supported by the National Institute of General Medical Sciences [GM119661].

Abbreviations

CL_{up}	antibody vascular fluid-phase endocytosis rate
CL_{IgG}	monoclonal antibody clearance
FcRn	neonatal Fc receptor
K_{on}	association rate constant;
K_{off}	dissociation rate constant;
mAb	monoclonal antibody
NCA	non-compartmental analysis
mPBPK	minimal physiologically based pharmacokinetic model
PBPK	physiologically based pharmacokinetic model
$T_{(W)}$	endosome transit time

ORCID

Brian M. Maas http://orcid.org/0000-0002-2410-4379
Yanguang Cao http://orcid.org/0000-0002-3974-9073

References

1. Ecker DM, Jones SD, Levine HL. The therapeutic monoclonal antibody market. MAbs. 2015;7(1):9–14. doi:10.4161/19420862.2015.989042.
2. Foltz IN, Karow M, Wasserman SM. Evolution and emergence of therapeutic monoclonal antibodies: what cardiologists need to know. Circulation. 2013;127(22):2222–2230. doi:10.1161/CIRCULATIONAHA.113.002033.
3. Wang W, Wang EQ, Balthasar JP. Monoclonal antibody pharmacokinetics and pharmacodynamics. Clin Pharmacol Ther. 2008;84(5):548–558. doi:10.1038/clpt.2008.170.
4. Ryman JT, Meibohm B. Pharmacokinetics of monoclonal antibodies. CPT Pharmacometrics Syst Pharmacol. 2017. doi: 10.1002/psp4.12224.
5. Gurbaxani B, Dostalek M, Gardner I. Are endosomal trafficking parameters better targets for improving mab pharmacokinetics than fcrn binding affinity? Mol Immunol. 2013;56(4):660–674. doi:10.1016/j.molimm.2013.05.008.
6. Dall'Acqua WF, Kiener PA, Wu H. Properties of human igg1s engineered for enhanced binding to the neonatal fc receptor (fcrn). J Biol Chem. 2006;281(33):23514–23524. doi:10.1074/jbc.M604292200.
7. Hinton PR, Xiong JM, Johlfs MG, Tang MT, Keller S, Tsurushita N. An engineered human igg1 antibody with longer serum half-life. J Immunol. 2006;176(1):346–356.
8. Yeung YA, Leabman MK, Marvin JS, Qiu J, Adams CW, Lien S, Starovasnik MA, Lowman HB. Engineering human igg1 affinity to human neonatal fc receptor: impact of affinity improvement on pharmacokinetics in primates. J Immunol. 2009;182(12):7663–7671. doi:10.4049/jimmunol.0804182.
9. Datta-Mannan A, Witcher DR, Lu J, Wroblewski VJ. Influence of improved fcrn binding on the subcutaneous bioavailability of monoclonal antibodies in cynomolgus monkeys. MAbs. 2012;4(2):267–273. doi:10.4161/mabs.4.2.19364.
10. Igawa T, Tsunoda H, Tachibana T, Maeda A, Mimoto F, Moriyama C, Nanami M, Sekimori Y, Nabuchi Y, Aso Y, et al. Reduced elimination of igg antibodies by engineering the variable region. Protein Eng Des Sel. 2010;23(5):385–392. doi:10.1093/protein/gzq009.
11. Acqua WFD, Woods RM, Ward ES, Palaszynski SR, Patel NK, Brewah YA, Wu H, Kiener PA, Langermann S. Increasing the affinity of a human igg1 for the neonatal fc receptor: biological consequences. J Immunol. 2002;169(9):5171–5180.
12. Ng CM, Fielder PJ, Jin J, Deng R. Mechanism-based competitive binding model to investigate the effect of neonatal fc receptor binding affinity on the pharmacokinetic of humanized anti-vegf monoclonal igg1 antibody in cynomolgus monkey. AAPS J. 2016;18(4):948–959. doi:10.1208/s12248-016-9911-4.
13. Borrok MJ, Wu Y, Beyaz N, Yu XQ, Oganesyan V, Dall'Acqua WF, Tsui P. Ph-dependent binding engineering reveals an fcrn affinity threshold that governs igg recycling. J Biol Chem. 2015;290(7):4282–4290. doi:10.1074/jbc.M114.603712.
14. Abdiche YN, Yeung YA, Chaparro-Riggers J, Barman I, Strop P, Chin SM, Pham A, Bolton G, McDonough D, Lindquist K, et al. The neonatal fc receptor (fcrn) binds independently to both sites of the igg homodimer with identical affinity. MAbs. 2015;7(2):331–343. doi:10.1080/19420862.2015.1008353.
15. Chen Y, Balthasar JP. Evaluation of a catenary pbpk model for predicting the in vivo disposition of mabs engineered for high-affinity binding to fcrn. AAPS J. 2012;14(4):850–859. doi:10.1208/s12248-012-9395-9.
16. Suzuki T, Ishii-Watabe A, Tada M, Kobayashi T, Kanayasu-Toyoda T, Kawanishi T, Yamaguchi T. Importance of neonatal fcr in regulating the serum half-life of therapeutic proteins containing the fc domain of human igg1: A comparative study of the affinity of monoclonal antibodies and fc-fusion proteins to human neonatal fcr. J Immunol. 2010;184(4):1968–1976. doi:10.4049/jimmunol.0903296.
17. Hopkins CR, Trowbridge IS. Internalization and processing of transferrin and the transferrin receptor in human carcinoma a431 cells. J Cell Biol. 1983;97(2):508–521.
18. Ober RJ, Martinez C, Vaccaro C, Zhou J, Ward ES. Visualizing the site and dynamics of igg salvage by the mhc class i-related receptor, fcrn. J Immunol. 2004;172(4):2021–2029.
19. Garg A, Balthasar JP. Physiologically-based pharmacokinetic (pbpk) model to predict igg tissue kinetics in wild-type and fcrn-knockout mice. J Pharmacokinet Pharmacodyn. 2007;34(5):687–709. doi:10.1007/s10928-007-9065-1.
20. Urva SR, Yang VC, Balthasar JP. Physiologically based pharmacokinetic model for t84.66: A monoclonal anti-cea antibody. J Pharm Sci. 2010;99(3):1582–1600. doi:10.1002/jps.21918.
21. Reverberi R, Reverberi L. Factors affecting the antigen-antibody reaction. Blood Transfus. 2007;5(4):227–240. doi:10.2450/2007.0047-07.
22. Cao Y, Jusko WJ. Survey of monoclonal antibody disposition in man utilizing a minimal physiologically-based pharmacokinetic model. J Pharmacokinet Pharmacodyn. 2014;41(6):571–580. doi:10.1007/s10928-014-9374-0.
23. Cao Y, Balthasar JP, Jusko WJ. Second-generation minimal physiologically-based pharmacokinetic model for monoclonal antibodies. J Pharmacokinet Pharmacodyn. 2013;40(5):597–607. doi:10.1007/s10928-013-9332-2.

24. Zhao J, Cao Y, Jusko WJ. Across-species scaling of monoclonal antibody pharmacokinetics using a minimal pbpk model. Pharm Res. 2015;32(10):3269–3281. doi:10.1007/s11095-015-1703-5.
25. Datta-Mannan A, Witcher DR, Tang Y, Watkins J, Jiang W, Wroblewski VJ. Humanized igg1 variants with differential binding properties to the neonatal fc receptor: relationship to pharmacokinetics in mice and primates. Drug Metab Dispos. 2007;35(1):86–94. doi:10.1124/dmd.106.011734.
26. Datta-Mannan A, Witcher DR, Tang Y, Watkins J, Wroblewski VJ. Monoclonal antibody clearance. Impact of modulating the interaction of igg with the neonatal fc receptor. J Biol Chem. 2007;282(3):1709–1717. doi:10.1074/jbc.M607161200.
27. Gill KL, Machavaram KK, Rose RH, Chetty M. Potential sources of inter-subject variability in monoclonal antibody pharmacokinetics. Clin Pharmacokinet. 2016;55(7):789–805. doi:10.1007/s40262-015-0361-4.
28. Datta-Mannan A, Wroblewski VJ. Application of fcrn binding assays to guide mab development. Drug Metab Dispos. 2014;42(11):1867–1872. doi:10.1124/dmd.114.059089.
29. Yuan D, Rode F, Cao Y. A minimal physiologically based pharmacokinetic model with a nested endosome compartment for novel engineered antibodies. AAPS J. 2018;20(3):48. doi:10.1208/s12248-017-0183-4.
30. Shah DK, Betts AM. Towards a platform pbpk model to characterize the plasma and tissue disposition of monoclonal antibodies in preclinical species and human. J Pharmacokinet Pharmacodyn. 2012;39(1):67–86. doi:10.1007/s10928-011-9232-2.
31. Hansen RJ, Balthasar JP. Effects of intravenous immunoglobulin on platelet count and antiplatelet antibody disposition in a rat model of immune thrombocytopenia. Blood. 2002;100(6):2087–2093.